Aqueous Gel Formation of a Synthetic Peptide Derived from the β-Sheet Domain of Platelet Factor-4

Nathan A. Lockwood,[†,‡] Robert van Tankeren,[†] and Kevin H. Mayo*[,†]

Department of Biochemistry, Molecular Biology & Biophysics, the Biomedical Engineering Center, and the Department of Chemical Engineering & Materials Science, University of Minnesota, Minneapolis, Minnesota 55455

Received May 17, 2002; Revised Manuscript Received September 3, 2002

We observed gelation of a 23-residue peptide derived from the β-sheet domain of platelet factor-4 ($PF4_{24-46}$). The gels were primarily heterogeneous mixtures of 50−200 μm spherical aggregates in a less-dense gel matrix. Infrared and circular dichroism spectroscopies showed gelation involving the conversion of $PF4_{24-46}$ from random coil to β-sheet. We used aggregation-induced NMR resonance broadening to show that temperature, pH, and ionic strength influenced $PF4_{24-46}$ gelation rates. Under identical solution conditions, gel formation took days at $T \leq 20$ °C but only 30 min at $T \geq 50$ °C. Gelation was most rapid at pH values near the pK_a of the central His35 residue. Increases in solution ionic strength reduced the critical gelation concentration of $PF4_{24-46}$. Our results suggest that $PF4_{24-46}$ gels by a process combining aspects of both heat-set and β-fibril gelation mechanisms.

Introduction

The phenomenon of biopolymer gelation is of current interest in many fields. In addition to scientific understanding of the gelation process, new materials are being developed via self-assembly and gelation,[1] and biocompatible gels are sought for applications in the fields of biomaterials, tissue engineering, and drug delivery.[2−4] Peptide-based materials have been shown to form aqueous gels with potential for biomedical and materials science applications.[4−7] In addition to the development of gel-based materials, interest in peptide assembly and gelation has grown because of the parallels drawn with the abnormal protein aggregation involved in Alzheimer's disease and Huntington's chorea.[8−11]

Biopolymer gelation typically follows one of two mechanisms. Heat-set biopolymer gels form when a solution of a protein (typically globular) is heated and subsequently cooled. The heating process induces a limited conversion from α-helix to β-sheet structure in the globular protein. This conformational change exposes hydrophobic residues, which create intermolecular links to form an extended, hydrated network of protein chains as the sample is cooled.[12,13] A measure of the secondary structure in this process shows an increase in coil and β-sheet content at the expense of α-helix during heating and little change on subsequent cooling.

In contrast, the gelation process in smaller gel-forming peptides appears to be a specific assembly of peptides into larger polymeric assemblies rather than nonspecific entanglements. This behavior is typically exhibited by β-sheet forming peptides, including de novo designed systems[1,6,14] and the β-amyloid peptides associated with development of Alzheimer's disease.[15] Assembly and gelation is characterized by hydrogen bonding between peptides to form extended intermolecular β-sheets that further associate into stacks of sheets, filaments, and fibrils as conformation shifts from coil to β-sheet.[1,8,9,16,17] The process occurs at a constant, often elevated, temperature but does not require cooling for intermolecular interactions to form the gel.

We have discovered the gelation of a peptide (residues 24−46) derived from the β-sheet domain of human platelet-factor 4 (PF4). PF4 is a 70-residue protein composed of a three-stranded antiparallel β-sheet domain onto which is folded a C-terminal α-helix and an aperiodic N-terminal region.[18,19] A number of biological functions have been attributed to PF4, including inhibition of the anticoagulant action of heparin and antiangiogenic activity via inhibition of endothelial cell proliferation.[20] The study of PF4 structure and function has led to many peptide derivatives serving as structural models of PF4 domains or functional analogues to the biological activities of PF4.[21−24] The gelation of $PF4_{24-46}$ was serendipitously observed during an NMR experiment examining the structure of the peptide.

In the present study, we investigated the gelation of $PF4_{24-46}$. We characterized the macroscopic and microscopic structures of $PF4_{24-46}$ gels via optical microscopy and environmental scanning electron microscopy. We used circular dichroism and infrared spectroscopies to assess peptide conformation before, during, and after gelation. To gain insight into the mechanism of gelation, we varied gelation conditions with respect to ionic strength, pH, peptide concentration, and temperature. To observe the rate of gelation under these conditions, we used NMR resonance broadening as a measure of aggregation, a technique that,

* To whom correspondence should be addressed. Department of Biochemistry, 6-155 Jackson Hall, University of Minnesota, 321 Church Street, Minneapolis, MN 55455. E-mail address: mayox001@umn.edu.

† Department of Biochemistry, Molecular Biology & Biophysics and the Biomedical Engineering Center.

‡ Department of Chemical Engineering & Materials Science.

10.1021/bm025573d CCC: $22.00
Published on Web 10/11/2002

to our knowledge, has not been used before in the assessment of gelation kinetics.

Experimental Section

Peptide Synthesis. The peptide representing amino acid residues 24 to 46 from human platelet factor-4, [ITSLEVIKAGPHSPTAQLIATLK-NH_2] ($PF4_{24-46}$,) was synthesized on a Milligen Biosearch 9600 automated peptide synthesizer following procedures based on Merrifield solid-phase synthesis with 9-fluorenylmethyloxycarbonyl (Fmoc) chemistry.[25] The C-terminus carboxylate group was synthesized in the amide form. The native C36 residue was replaced by serine to avoid complications with cysteine oxidation. The peptide support and side chain protecting groups were cleaved with a mixture of trifluoroacetic acid and scavengers following synthesis. Crude peptide was purified on a preparative reverse-phase HPLC Vydac C_{18} column using an elution gradient of 0−60% acetonitrile with 0.1% trifluoroacetic acid in water. The purified peptide was analyzed for amino acid composition on a Beckman 6300 amino acid analyzer by total hydrolysis (6N HCl at 110 °C for 18−20 h) and by mass spectrometry. The final peptide purity was greater than 95%.

Optical Photography & Microscopy. Photographs of $PF4_{24-46}$ gels in inverted 5 mm NMR tubes were taken with a Kodak digital camera. Phase-contrast optical micrographs of $PF4_{24-46}$ gels were taken with a Nikon Eclipse TS100 inverted microscope (10× objective). Images were captured using a CCD camera with Scion Image software. All digital images were processed in Adobe Photoshop.

Environmental Scanning Electron Microscopy. Environmental scanning electron microscopy (ESEM) micrographs were obtained with a Philips Electroscan environmental scanning electron microscope. Hydrated $PF4_{24-46}$ gels were imaged without special sample preparation (e.g., critical-point drying and coating with gold) in a water-saturated atmosphere at 4 °C. ESEM images were taken at various states of dehydration to visualize gel structures and identify dehydration artifacts.

Circular Dichroism. Peptides for circular dichroism (CD) were dissolved in water at 1 or 24 mg/mL with 10 mM NaCl and pH-adjusted with NaOH. CD spectra were measured on a Jasco J-710 spectropolarimeter coupled to a data processor. Spectra were recorded digitally and fed through the data processor for signal averaging, baseline subtraction, and noise reduction. CD spectra were recorded from 190 to 250 nm using a 0.1 mm path-length, thermally jacketed quartz cuvette maintained at 50 °C with a NesLab water bath. The step resolution was 0.1 nm, scan speed was 50 nm/min, response time was 1 s, and sensitivity was 100 mdeg. CD spectra were fit with a linear combination of standard secondary spectra to estimate secondary structure contributions.[26]

Infrared Spectroscopy. Fourier transform infrared (FTIR) spectra were recorded on a Nicolet Magna 750 spectrometer equipped with a liquid nitrogen cooled mercury/cadmium telluride (MCT) detector at 4 cm^{-1} resolution. Samples of completely formed gels were placed in a liquid cell with CaF_2 crystal windows and a 15 μm Teflon spacer for measurement. Spectra were recorded at 20 °C and averaged over 1024 solvent-subtracted scans.

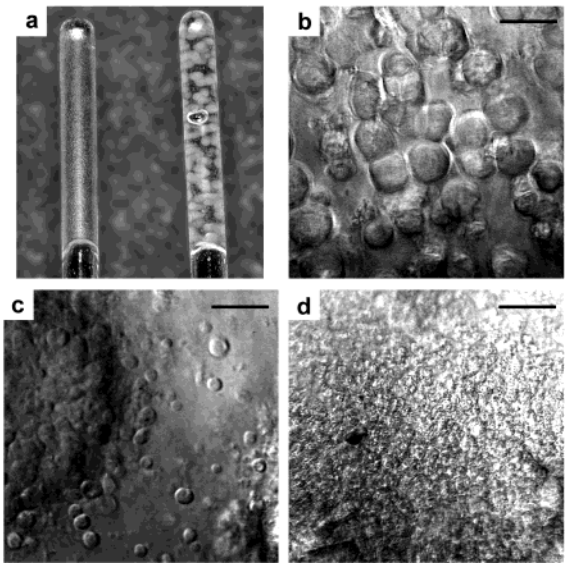

Figure 1. Photograph (a) of two inverted $PF4_{24-46}$ gels (24 mg/mL, 10 mM NaCl, pH 4.1 (left) and pH 5.6 (right)) demonstrating lack of fluidity. Also visible is the agglomeration of clear particles into larger, opaque aggregates (right). Tubes are 5 mm wide. Panels b−d show optical micrographs of $PF4_{24-46}$ gels (24 mg/mL, 10 mM NaCl) at pH (b) 4.1, (c) 5.6, and (d) 9.6. Gels were typically heterogeneous, containing transparent spherical particles in a clear matrix. Aggregates of these particles were observed in some samples (left portion of panel c). Scale bars are 250 μm.

Gelation Kinetics via NMR. NMR experiments were performed on Varian UNITY-Plus 500 or 600 NMR spectrometers. For NMR samples, freeze-dried peptides were dissolved in either D_2O or 9:1 H_2O/D_2O and pH-adjusted with NaOD or DCl. NaCl concentrations ranged from zero (none added) to 100 mM. NMR measurements were made on the samples immediately after preparing the solutions to try to capture early kinetic events. The typical time between sample preparation and the first NMR spectrum was 20 min because of instrument shimming and tuning. Kinetic processes were measured as the drop in resonance intensity (due to broadening) in the NMR spectrum over time. Kinetics were visualized by plotting the change in amplitude as the fraction $I(t)/I_0$.

Results & Discussion

General Observations. We first observed gelation of $PF4_{24-46}$ as a simple lack of fluidity in an NMR sample (Figure 1a). $PF4_{24-46}$ gel samples were typically heterogeneous in nature, consisting of opaque to transparent spherical aggregates in a transparent matrix. All of the gels that we observed contained some level of heterogeneity, though the size scale of the more optically dense aggregates depended on gelation conditions. Under conditions that produced very large opaque aggregates, some fluidity was observable in the surrounding matrix, although the matrix remained viscous enough to prevent the aggregates from settling to the bottom of the tube.

Optical micrographs showed that gels were heterogeneous in nature, formed primarily of 45−160 μm particles and

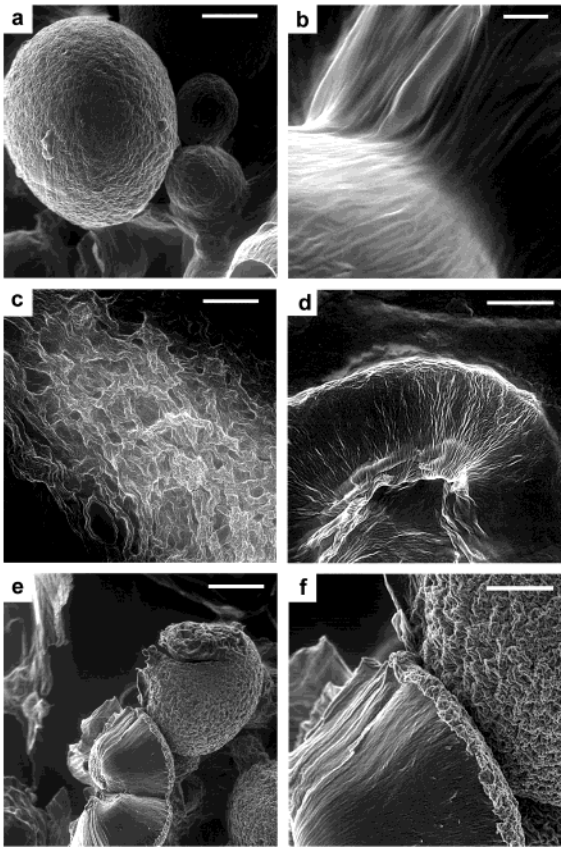

Figure 2. Environmental SEM micrographs of $PF4_{24-46}$ gels. Structures were typically 50−250 μm spheres in a less-dense matrix (panels a and b) or coarse networks (panels c and d). During prolonged time in the ESEM, gels dehydrated and spherical aggregates burst (panels e and f), revealing a radial inner structure. Conditions were as follows: (a, b, e, f) 30 mg/mL $PF4_{24-46}$, pH 5.7, 10 mM NaCl; (c, d) 24 mg/mL $PF4_{24-46}$, pH 4.1, 10 mM NaCl. Scale bars are (a, c, e) 100, (b) 10, and (d, f) 40 μm.

millimeter-sized aggregates in a less-dense matrix (Figure 1b−d.) At high and low pH, gels were typically more uniform in macroscopic appearance than at pH values between 5.5 and 7.0 and microscopically showed a fairly uniform distribution of spherical particles. At pH conditions near 5.5−6.5, the spherical particles agglomerated to form large opaque aggregates (visible in the left portion of Figure 1c) with fewer disaggregated transparent particles.

We used environmental SEM (ESEM) to gain a more detailed view of the types of microscopic structures present in $PF4_{24-46}$ gels (Figure 2). The relatively high water vapor pressure in ESEM permits imaging of the surfaces of hydrated samples. ESEM images of $PF4_{24-46}$ gels showed heterogeneous microstructures, typically consisting of 50−300 μm spherical particles (Figure 2a,b.) A few samples showed a more uniform network microstructure lacking both the small particles and large aggregates (Figure 2c,d.) This network was composed of 10−20 μm diameter domains in a fairly isotropic, branched microstructure. The domains observed are too large to be composed of single peptide fibrils and are likely a result of phase separation under these pH conditions rather than a reflection of fibrous assembly.

While the dominant microstructural feature of $PF4_{24-46}$ gels is the spherical or network phase separation, we observed some features suggesting oriented growth in the gels. Higher magnification images revealed an oriented texture perpendicular to the "macrofiber" direction in the network gels (Figure 2d) and extending radially in fractured spherical particles (Figure 2e,f.) We were unable to image these textured regions in any greater detail because of artifacts created by further dehydration. However, the $PF4_{24-46}$ microstructure showed distinct differences from other synthetic β-sheet gel-forming peptides, which form extended tape architectures[1] or helical assemblies.[27]

We also used ESEM to probe the development of $PF4_{24-46}$ aggregates during the course of gelation, but the results of these experiments did not provide information at the level of detail that we had hoped. At long times (>200 min), we observed structures such as those shown in Figure 2. Images taken at early (40−50 min) and intermediate (100−150 min) times showed either a lack of aggregates or large aggregates similar to those of the final gel state. However, the search for aggregates in these samples required high levels of dehydration. This, combined with the high concentration of $PF4_{24-46}$ in solution, led us to fear that the majority of what we observed were artifacts of $PF4_{24-46}$ aggregation during dehydration rather than true gel aggregates.

Gel Structure and Development at the Molecular Level. We compared the solution structure of $PF4_{24-46}$ at subgelling concentrations with that of the gelled peptide using circular dichroism (CD), a method commonly used to assess the conformational distribution of peptides in solution.[28,29] At low concentration (1 mg/mL), $PF4_{24-46}$ yielded a CD spectrum consistent with a primarily coiled structure or an interconverting array of secondary structures with a trough near 198 nm and a shoulder near 220 nm (Figure 3a). A linear combination of standard secondary structure basis spectra (α-helix, β-sheet, random coil) fit to the 1 mg/mL $PF4_{24-46}$ spectrum yielded 68% coil and 28% β-sheet. This is consistent with other work characterizing the solution structure of $PF4_{24-46}$.[22,30] CD spectra of 1 mg/mL $PF4_{24-46}$ solutions at 50 °C were similar to those at 20 °C (data not shown). The CD spectrum of $PF4_{24-46}$ in the gel state (24 mg/mL) showed a much greater fraction of β-sheet (98%.) Absorbance from the peptide and scattering from gel aggregates limited useful CD data to wavelengths greater than 205 nm. Consequently, the fit of the spectrum excluded data below 205 nm, leading to a possible overestimate of β-sheet in the sample. While the exclusion of such data may have increased the numerical error in β-sheet estimation, the shape of the spectrum above 205 nm was clearly consistent with β-sheet structure, showing a broad trough at 217 nm.[29,31]

We verified our characterization of β-sheet in the final gel state with infrared (IR) spectroscopy. A strong IR band for β-sheet structure is found at 1612−1640 cm^{-1} and a weaker one at 1670−1690 cm^{-1}, whereas IR bands for α-helix and random coil both lie in the 1640−1660 cm^{-1} range.[32−34] IR spectra of $PF4_{24-46}$ gels confirmed the presence of β-sheet structure (Figure 3b); IR bands were observed at 1614, 1677, and 1689 cm^{-1}. No significant α-helix or random coil IR bands were observed.

The differences that we observed between the CD spectra of $PF4_{24-46}$ in the gel and solution states prompted us to examine the evolution of CD spectra during gelation of

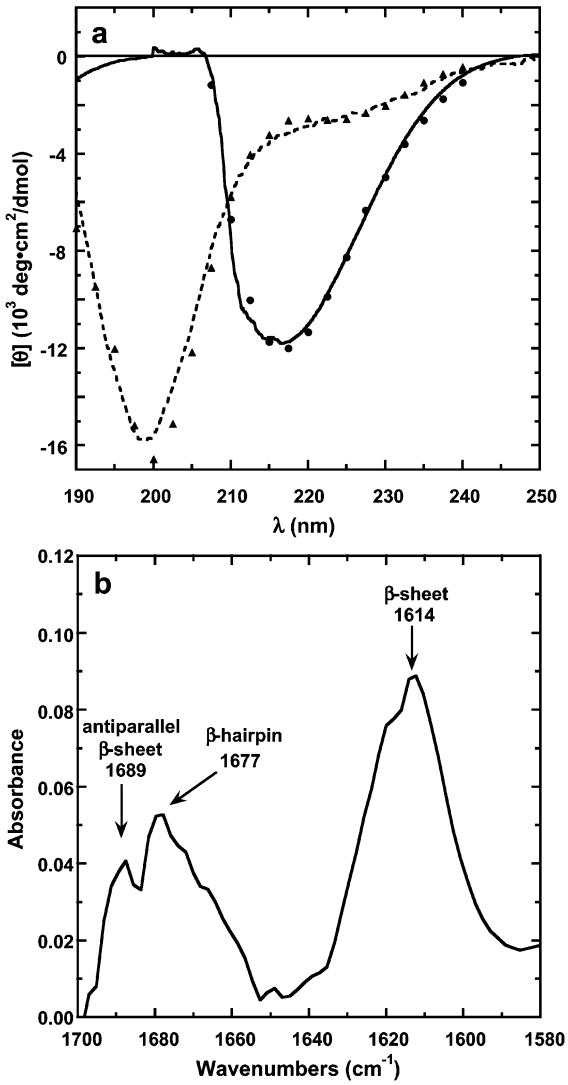

Figure 3. CD spectra (a) of $PF4_{24-46}$ in 10 mM NaCl, pH 4.1, at a nongelling concentration (1 mg/mL, 20 °C, dotted line) and in the final gel state (24 mg/mL, 50 °C gel temperature, solid line.) A fit to the dilute $PF4_{24-46}$ spectrum (▲) yielded 68% random coil, 28% β-sheet, and 4% α-helix. A fit to the $PF4_{24-46}$ gel spectrum at $\lambda \geq 205$ nm (●) gave 98% β-sheet, 2% random coil. Panel b shows the FTIR spectrum of the final state of $PF4_{24-46}$ gel (24 mg/mL, 10 mM NaCl, pH 7.0, 50 °C gel temperature.) Labeled bands are consistent with β-sheet structure; bands for helix and coil were not observed. Spectra of gels produced under other solution conditions were similar.

$PF4_{24-46}$ at 50 °C (Figure 4). These spectra, like that of the final gel state, suffered from absorption and scattering problems, limiting useful CD data to that above 210 nm. However, data above 210 nm were sufficient to see structure development during $PF4_{24-46}$ gelation. At the first time point (13 min after sample preparation, 1−2 min after reaching 50 °C), the CD trace was consistent with the absence of significant β-sheet or α-helical conformation. Over the course of several hours, the shoulder near 220 nm evolved into a 217 nm β−sheet trough. The shape change of the spectra was observed for all samples, although the spectra often decreased in intensity during gelation, probably the result of light scattering from the aggregated peptide.

Our CD data create a picture of gelation in which the solvated $PF4_{24-46}$ peptide starts as a random coil or an array of interconverting conformations. Once the gelation process

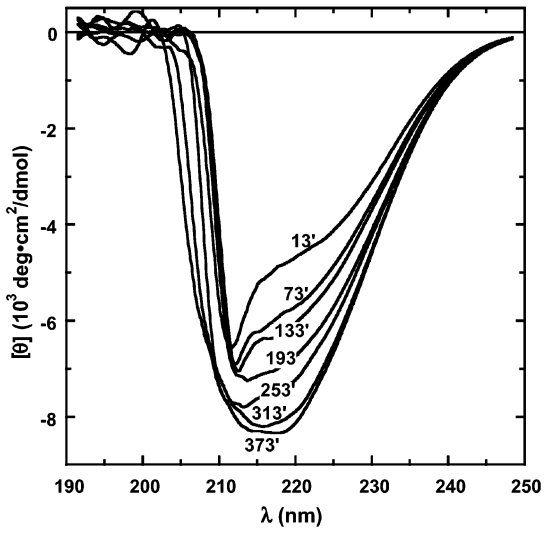

Figure 4. Evolution of CD spectra during $PF4_{24-46}$ gelation at 50 °C. Spectra shown are typical, indicating an increase in β-sheet secondary structure over several hours. Spectra often decreased in intensity with time because of scattering from the gel aggregates; the spectra beyond 193 min were scaled in this figure such that they did not overlap.

begins, the $PF4_{24-46}$ peptides incorporated into the gel state take on a primarily β-sheet conformation, suggesting that the gel state stabilizes β-sheet secondary structure in some manner. The presence of β-sheet structure in the gelled $PF4_{24-46}$ peptide echoes the antiparallel β-sheet conformation of residues 24−46 in the full-length PF4 protein.[35] The development of structure concomitant with gelation has been observed in other gel-forming peptide systems, particularly in peptides with a propensity for β-sheet structure.[1,8,9,14,16,17]

Kinetics of Gelation. We used 1D ^{1}H NMR spectroscopy to monitor gelation kinetics in the $PF4_{24-46}$ system by observing the reduction in NMR signal intensity due to resonance broadening during the course of $PF4_{24-46}$ gelation (Figure 5). As peptide molecules aggregate into a gel, they become immobilized and produce highly broadened NMR resonances that contribute only marginally to the spectrum.[36] Resonances that are still observed are associated with free peptide not yet incorporated into the gel,[37] although diffusional restrictions within or between gel particles or both may also cause free peptide resonances to broaden somewhat. When normalized by the initial resonance intensity (that of bulk free peptide), resonance intensity yields the fraction of peptide in the disaggregated state. As far as we know, this is a new method for studying gelation, although other types of NMR experiments have been used to study biopolymer gels.[9,37−39]

For kinetic measurements, we plotted normalized signal intensity vs time, using the intensity of the 1.08 ppm resonance for all measurements. Results for other resonances (1.5, 3.5, 7.4 ppm) were consistent with those observed at 1.08 ppm. For simplicity in making comparisons between NMR experiments, we define a value $t_{1/2}$ as the time at which the NMR resonance intensity decreases to 50% of its original value.

Effect of Gelation Temperature. When $PF4_{24-46}$ gelation was initially discovered, it appeared that gelation occurred

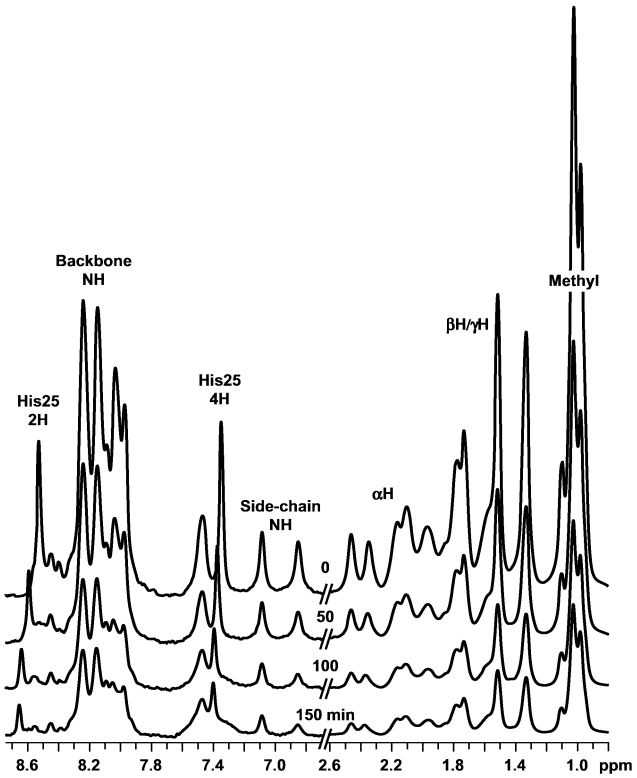

Figure 5. A series of ^{1}H NMR spectra obtained during gelation of $PF4_{24-46}$ at 50 °C (24 mg/mL, 10 mM NaCl, pH 5.6). Only the downfield region, 6.7 to 8.7 ppm, and upfield region, 2.6 to 0.8 ppm, are displayed to simplify the spectra. The decrease in resonance intensity and concomitant resonance broadening are a result of the association of $PF4_{24-46}$ peptides into slow-tumbling aggregates. We used this change in spectral intensity as a measure of aggregation and gelation.

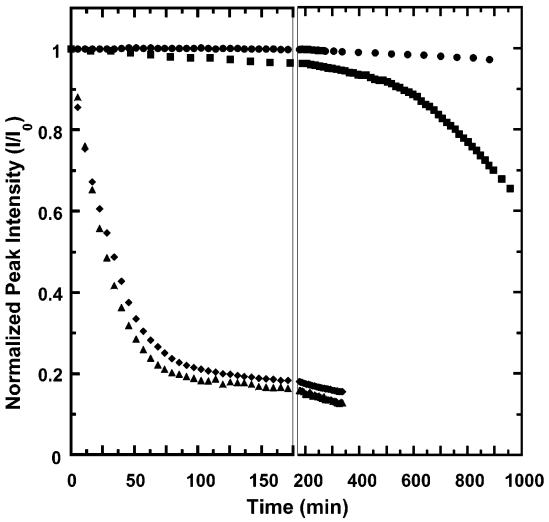

Figure 6. $PF4_{24-46}$ (24 mg/mL,10 mM NaCl, pH 6.7) NMR resonance broadening at gelation temperatures of (●) 4, (■) 20, (◆) 50, and (▲) 60 °C. No resonance broadening or gelation was observed at 4 °C up to 900 min. At 20 °C, resonance broadening indicates gelation started near 400 min with $t_{1/2}$ greater than 1000 min. Resonance broadening at 50 and 60 °C, started immediately and completed by 125 min ($t_{1/2}$ = 32 and 26 min for 50 and 60 °C, respectively).

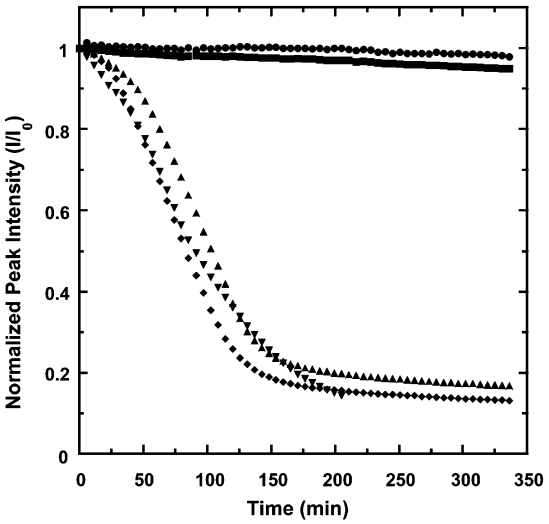

Figure 7. NMR resonance broadening during gelation of (●) 10, (■) 15, (◆) 20, (▲) 24, and (▼) 30 mg/mL $PF4_{24-46}$ under identical solution conditions (pH 5.7, 10 mM NaCl, 50 °C gelation temperature.) At the two lowest concentrations, no gelation was observed, as shown by the lack of NMR resonance broadening. Samples at 20, 24, and 30 mg/mL showed a characteristic decrease in their NMR resonance intensities (a reflection of resonance broadening) indicative of gel formation. The critical gel concentration for $PF4_{24-46}$ at pH 5.7, 10 mM NaCl, lies between 15 and 20 mg/mL. The plateau beyond 200 min indicates 10−20% residual free peptide for the 20, 24, and 30 mg/mL concentrations.

only at elevated temperatures and that cooling was not required for gel formation. To verify this qualitative observation, we investigated the effect of temperature on $PF4_{24-46}$ gelation via NMR resonance broadening at 24 mg/mL, 10 mM NaCl, pH 5.7 (Figure 6). At 4 °C, NMR spectra showed only minor intensity changes over the course of 1000 min, suggesting no development of gel aggregates. In fact, solutions stored at 4 °C showed no qualitative signs of gelation even when stored for several days. At 20 °C, NMR spectra showed a similar minor, slow intensity decrease for the first 500 min, followed by a more rapid decrease in intensity with an estimated $t_{1/2}$ above 1000 min. This behavior is in sharp contrast to $PF4_{24-46}$ solutions gelled at 50 and 60 °C. At these temperatures, no slow initial intensity decrease was observed; resonances quickly broadened, yielding $t_{1/2}$ values of 32 and 26 min for 50 and 60 °C, respectively. It is likely that the kinetics in these cases are sufficiently fast that the slow phase (if any) was completed before the instrument was set up to acquire spectra (instrument setup typically took 20 min after the sample was placed in the magnet).

Effect of $PF4_{24-46}$ Concentration. We observed no gelation in $PF4_{24-46}$ solutions prepared at 1 mg/mL, while solutions prepared at higher concentrations formed gels. To better understand this, we measured gelation kinetics via NMR resonance broadening for concentrations ranging from 10 to 30 mg/mL to determine whether a critical gel concentration existed at pH 5.7, 10 mM NaCl, and 50 °C gelation temperature (Figure 7). At 10 and 15 mg/mL, NMR resonance intensity decreased slightly (ca. 2−5% drop in 360 min), but no clear gel transition was apparent from the NMR data. This was supported by the fact that the samples remained fluid after the experiment. For 10 and 15 mg/mL samples, $t_{1/2}$ was greater than the time of our experiment. The NMR resonance broadening for 20, 24, and 30 mg/mL $PF4_{24-46}$ samples was different from that observed at lower

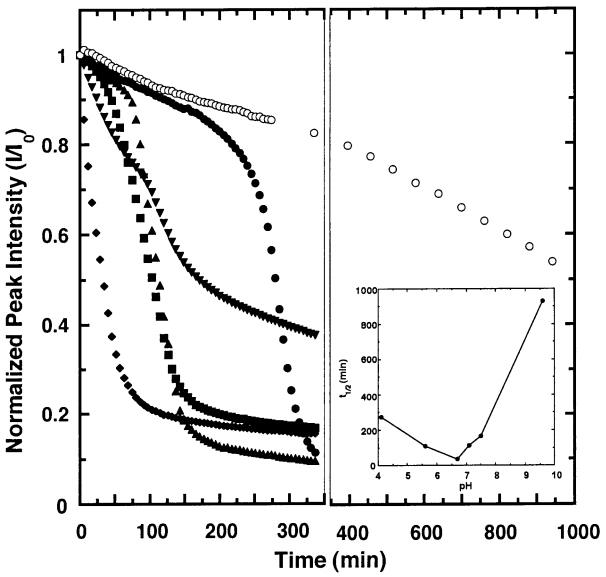

Figure 8. NMR resonance broadening of $PF4_{24-46}$ gelation (24 mg/mL, 10 mM NaCl, 50 °C gelation temperature) at pH (●) 4.1, (■) 5.6, (◆) 6.7, (▲) 7.0, (▼) 7.5, and (○) 9.6. Resonance broadening indicated gel formation at all pH values. The rate of gelation was slowest at high or low pH and increased near pH 6.7, as shown by comparison of $t_{1/2}$ values (inset).

concentrations. NMR resonances broadened rapidly, reaching a low plateau within 200 min. These three concentrations showed similar $t_{1/2}$ values (84, 103, and 92 min for 20, 24, and 30 mg/mL, respectively). All of the samples at 20, 24, and 30 mg/mL lacked fluidity when removed from the NMR spectrometer, although the plateau in NMR resonance intensity at longer times suggests that only 80−90% of the $PF4_{24-46}$ was incorporated into the gel state. These results place the critical gel concentration for $PF4_{24-46}$ in 10 mM NaCl, pH 5.7, somewhere between 15 and 20 mg/mL. We note that the critical gel concentration for $PF4_{24-46}$ is consistent with values for the critical gel concentration measured for other peptide and protein systems, which typically fall in the range of 1−50 mg/mL.[1,40]

Role of Electrostatics. Given the highly charged nature of $PF4_{24-46}$, we hypothesized that electrostatics play an important role in both the development of gels and the kinetics of gel formation. The two primary methods of varying electrostatics of peptide interactions are via pH changes (varying the degree of peptide charge) and solution ionic strength (altering the screening of charges on the peptide). We again used NMR resonance broadening to study gelation kinetics in $PF4_{24-46}$ solutions (10 mM NaCl, 50 °C gelation temperature) at pH 4.1, 5.6, 6.7, 7.0, 7.5, and 9.6 (Figure 8). Resonance broadening was most rapid at pH 6.7 ($t_{1/2} = 34$ min) and slowed as the pH was either increased or decreased (Figure 8, inset). At pH 9.6, resonance broadening was particularly slow ($t_{1/2} \approx 1000$ min), although the sample did form a gel. These data indicate that the distribution of charged groups on the peptide (E28, H35, K31, K46, and the N-terminus) affected gelation. It would seem that the minimal $t_{1/2}$ (fastest gelation) would occur at a pH close to the isoelectric point (p*I*) of $PF4_{24-46}$. However, the calculated p*I* of $PF4_{24-46}$ is 9.9, close to the pH at which we measured the slowest gelation kinetics. In fact, the actual

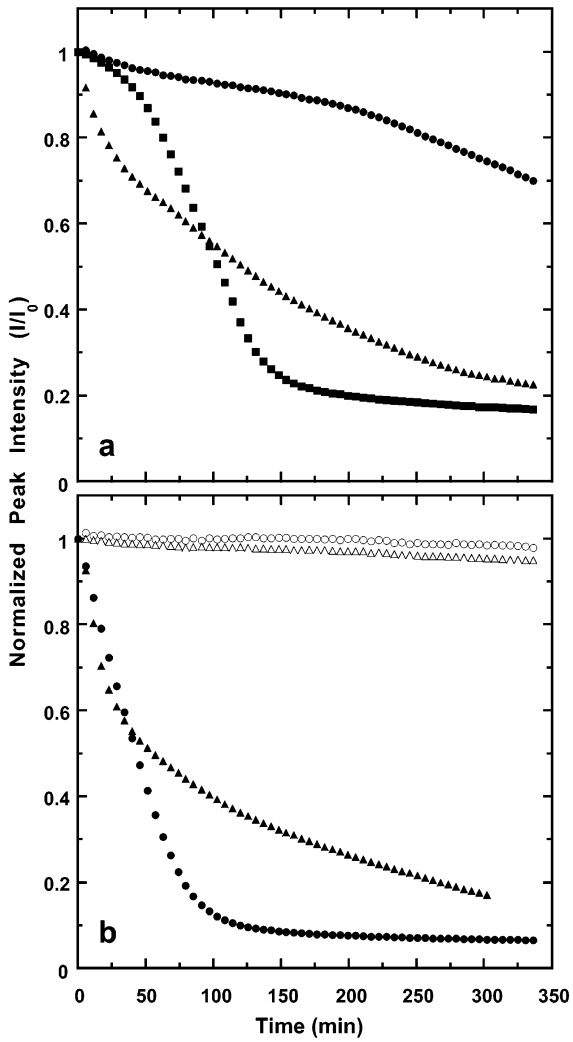

Figure 9. NMR resonance broadening (a) of $PF4_{24-46}$ solutions (24 mg/mL, pH 5.6, 50 °C gel temperature) containing (●) 0 (none added), (■) 10, or (▲) 100 mM NaCl. With no added salt, resonance broadening indicated slow gelation with $t_{1/2}$ greater than 350 min. Addition of 10 mM NaCl showed an increased rate of gelation ($t_{1/2} =$ 45 min), and 100 mM NaCl yielded a different functional form of the curve with a faster initial gelation rate but an intermediate rate at longer times. Panel b shows NMR resonance broadening of $PF4_{24-46}$ (pH 5.9, 50 °C gel temperature) at (○,●) 10 or (△,▲) 15 mg/mL. Resonance broadening indicated no gelation at (○,△) 10 mM NaCl, while an increase to (●,▲) 100 mM NaCl induced gelation in both samples. The shape of the 15 mg/mL, 100 mM NaCl, curve also showed a more gradual transition.

p*I* is likely higher than 9.9 because the calculation assumes an acid C-terminus and we synthesized the C-terminus of $PF4_{24-46}$ in amidated form. The pK_a of His35 is probably near 6.1,[41] suggesting that the charge of His35 may play some role in $PF4_{24-46}$ gelation. It is interesting to note that while most resonances were not chemically shifted over time, those arising from His35 side chain 2H and 4H resonances were exceptions (Figure 5). Histidine side-chain resonances are known to be quite sensitive to pH;[42] the downfield shift suggests that His35 became more protonated because of a small decrease in solution pH during gelation. This shift seems to support the idea that the charge state of His35 influences the gelation process.

As another measure of electrostatic effects, we varied the ionic strength of $PF4_{24-46}$ solutions (Figure 9a). At a $PF4_{24-46}$

concentration of 24 mg/mL, gelation kinetics were relatively slow when no NaCl was added to the sample ($t_{1/2}$ = 400 min); in the presence of 10 mM NaCl, the gelation rate increased ($t_{1/2}$ = 45 min). Addition of 10-fold more salt (100 mM NaCl) yielded an intermediate rate of gelation ($t_{1/2}$ = 120 min) but also changed the shape of the gelation profile. A similar effect was observed for samples prepared with $PF4_{24-46}$ concentrations below the critical gel concentration at 10 mM NaCl (Figure 9b). Following the initial experiment at 10 mM NaCl, the samples were removed from the NMR and a sufficient amount of 1 M NaCl was added to bring the final concentration to 100 mM NaCl. This also created a minor (~9%) reduction in the concentration of $PF4_{24-46}$. The sample was placed back into the NMR for continued measurement. NMR resonance broadening indicated gelation at 10 and 15 mg/mL $PF4_{24-46}$ in the presence of 100 mM NaCl, despite the fact that neither of these concentrations formed gels at 10 mM NaCl. The shape of the NMR resonance broadening for 15 mg/mL was similar to that of the 100 mM NaCl, 24 mg/mL condition (Figure 9a).

The change in the functional form of the gelation curve makes direct comparison of $t_{1/2}$ values insufficient to characterize the effects of solution ionic strength. A better comparison may be the initial slopes of the gelation curves, which show the relative gelation rates to be 100 > 10 > 0 mM NaCl. On the basis of this comparison, the influence of solution ionic strength is as expected for a system in which like-charged particles assemble into larger aggregates. Increases in solution ionic strength cause more effective screening of the charge−charge repulsion between aggregating peptides. This reduces the kinetic barrier to assembly, leading to more rapid initial rates of gelation.[43] The observation that the functional form of the gelation curve changes for certain combinations of $PF4_{24-46}$ and NaCl concentrations suggests that there were at least two different mechanisms of gelation present in the $PF4_{24-46}$ system. Under conditions of moderate salt, the gelation appeared to be cooperative in nature with a sharp transition from free to aggregated peptide. Under conditions of high salt and above a threshold $PF4_{24-46}$ concentration, the gelation mechanism appeared to be less cooperative, displaying a broader transition from free to aggregated peptide.

Our experiments with variations in pH and ionic strength indicate that electrostatics play a prominent role in the aggregation and gelation of $PF4_{24-46}$. There also appears to be an interplay between the concentration of $PF4_{24-46}$ and ionic strength of the solution such that the critical gelation concentration varies with ionic strength. A similar relationship between ionic strength and critical gelation concentration has been observed in the gelation of β-lactoglobulin.[40] Our observation that low $PF4_{24-46}$ concentrations (10−15 mg/mL) require a higher ionic strength to form gels is akin to more detailed measurements on a 12-residue synthetic β-sheet peptide gel system,[44] the behavior of which is essentially consistent with the predictions of the Derjaguin−Landau−Verwey−Overbeek theory of interaction forces.[45,46]

Comparison to Other Gel-Forming Biopolymers. We have examined $PF4_{24-46}$ gelation at the macroscopic and molecular levels and found (1) a typically spherical phase-separated gel morphology, (2) β-sheet formation concomitant with gelation, (3) gel formation at elevated temperatures (≥50 °C), and (4) electrostatic influence on the rate of gelation. In comparison of these results with the behavior of other biopolymer gels, the mechanism of $PF4_{24-46}$ gelation appears to be a combination of heat-set and fibril-forming gelation behavior.

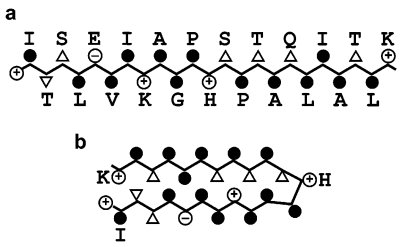

Figure 10. $PF4_{24-46}$ sequence schematics showing hydrophobic (●), polar (△,▽), and charged residues. The N-terminal charge is also shown. Panel a shows $PF4_{24-46}$ in an extended β-strand conformation; panel b shows $PF4_{24-46}$ in an antiparallel β-sheet conformation based on NMR structures of the full-length PF4 protein.[35]

The phase separation, overall isotropic gel microstructure (i.e., lack of fine-stranded assemblies), and high gelation concentration that we observed in the $PF4_{24-46}$ system show similarities to heat-set globular protein gels.[12,13] However, the mechanism of gelation must differ on a fundamental level because $PF4_{24-46}$ formed gels at elevated temperatures independent of the subsequent cooling required for heat-set gels. Our CD results showed a shift from a primarily coil to β-sheet conformation during $PF4_{24-46}$ gelation, distinctly different from the helix to coil/sheet observed in heat-set gel systems. The small size of $PF4_{24-46}$ may be one reason for differences between heat-set and $PF4_{24-46}$ gelation. The lack of globular structure makes it unlikely that $PF4_{24-46}$ could follow the heat-set pathway of unfolding and entanglement.

In terms of molecular size, $PF4_{24-46}$ has much more in common with the β-sheet fibril-forming gels than with globular proteins. The β-sheet formation that we observed during $PF4_{24-46}$ gelation shows a strong resemblance to β-sheet development in fibril-forming gels.[1,9] However, our ESEM analysis of $PF4_{24-46}$ gels show a different microstructural behavior than that of most fibril-forming gels. $PF4_{24-46}$ showed a dominantly spherical microstructure, whereas β-amyloid and related designed peptides are composed of long filaments and fibrils at the microstructural level.[15,17,27]

In terms of sequence and β-sheet structure, the sequence of $PF4_{24-46}$ shows some similarities to other β-forming peptides (Figure 10a): one face of the β-strand is dominantly hydrophobic, while the other is primarily hydrophilic. This is also true for the $PF4_{24-46}$ sequence in an the antiparallel β-sheet conformation; the sequence is in the parent protein (Figure 10b).[35] The hydrophobic nature of the peptide may drive the phase separation that we observed, and the interactions between charged residues (the peptide has an overall positive charge at all pH conditions that we investigated) may counter the hydrophobic phase separation. Our observation that the fastest gel kinetics occurred near the pK_a of the central histidine residue suggests that it plays some

role, either at the center of the peptide in an extended β-sheet or at the end of a turn in an antiparallel β-sheet.

Conclusion

We have discovered gelation in $PF4_{24-46}$, a β-sheet-forming peptide derived from human platelet factor-4. Our results showed that $PF4_{24-46}$ exhibits macro- and microscopic behaviors similar to heat-set globular protein gels, with phase separation apparent during gelation. On a molecular scale, our results showed that $PF4_{24-46}$ develops β-sheet conformation during the course of gelation, a property commonly seen in β-fibril-forming gels. The discovery of a peptide gel with such intermediate properties contributes to the greater literature on protein and peptide gelation. In addition, the gel nature of $PF4_{24-46}$ suggests properties useful for application to biomedical problems such as tissue replacement or wound therapy.

Acknowledgment. We are grateful to Dinesha S. Walek at the University of Minnesota Microchemical Facility for her expertise in peptide synthesis and to Dr. Stuart McKernan at the University of Minnesota Characterization Facility for his assistance with ESEM. We thank Raymond Tu, Dr. Ryan Toomey, and Dr. Matthew Tirrell for their helpful comments on the manuscript. This work was supported by a research grant from the Department of Defense (Army) to K.H.M. (Grant DAMD17-99-1-9564.) N.A.L. was supported by a Whitaker Foundation Graduate Fellowship. NMR instrumentation was provided with funds from the NSF (Grant BIR-961477), the University of Minnesota Medical School, and the Minnesota Medical Foundation.

References and Notes

(1) Aggeli, A.; Bell, M.; Boden, N.; Keen, J. N.; McLeish, T. C. B.; Nyrkova, I.; Radford, S. E.; Semenov, A. *J. Mater. Chem.* **1997**, *7*, 1135.
(2) Lee, K. Y.; Mooney, D. J. *Chem. Rev.* **2001**, *101*, 1869.
(3) Holmes, T. C.; de Lacalle, S.; Su, X.; Liu, G.; Rich, A.; Zhang, S. *Proc. Natl. Acad. Sci. U.S.A.* **2000**, *97*, 6728.
(4) Tan, M. M.; Corley, C. A.; Stevenson, C. L. *Pharm. Res.* **1998**, *15*, 1442.
(5) McMillan, R. A.; Conticello, V. P. *Macromolecules* **2000**, *33*, 4809.
(6) Leon, E. J.; Verma, N.; Zhang, S.; Lauffenburger, D. A.; Kamm, R. D. *J. Biomater. Sci., Polym. Ed.* **1998**, *9*, 297.
(7) Kirschner, D. A.; Inouye, H.; Duffy, L. K.; Sinclair, A.; Lind, M.; Selkoe, D. J. *Proc. Natl. Acad. Sci. U.S.A.* **1987**, *84*, 6953.
(8) Aggeli, A.; Nyrkova, I. A.; Bell, M.; Harding, R.; Carrick, L.; McLeish, T. C. B.; Semenov, A. N.; Boden, N. *Proc. Natl. Acad. Sci. U.S.A.* **2001**, *98*, 11857.
(9) Lyon, R. P.; Atkins, W. M. *J. Am. Chem. Soc.* **2001**, *123*, 4408.
(10) Janek, K.; Behlke, J.; Zipper, J.; Fabian, H.; Georgalis, Y.; Beyermann, M.; Bienert, M.; Krause, E. *Biochemistry* **1999**, *38*, 8246.
(11) Takahashi, Y.; Ueno, A.; Mihara, H. *Bioorg. Med. Chem.* **1999**, *7*, 177.
(12) Clark, A. H.; Kavanagh, G. M.; Ross-Murphy, S. B. *Food Hydrocolloids* **2001**, *15*, 383.
(13) Gosal, W. S.; Ross-Murphy, S. B. *Curr. Opin. Colloid Interface Sci.* **2000**, *5*, 188.
(14) Zhang, S.; Holmes, T.; Lockshin, C.; Rich, A. *Proc. Natl. Acad. Sci. U.S.A.* **1993**, *90*, 3334.
(15) Serpell, L. C. *Biochim. Biophys. Acta* **2000**, *1502*, 16.
(16) Aggeli, A.; Bell, M.; Boden, N.; Keen, J. N.; Knowles, P. F.; McLeish, T. C. B.; Pitkeathly, M.; Radford, S. E. *Nature* **1997**, *386*, 259.
(17) Aggeli, A.; Fytas, G.; Vlassopoulos, D.; McLeish, T. C. B.; Mawer, P. J.; Boden, N. *Biomacromolecules* **2001**, *2*, 378.
(18) Deuel, T. F.; Keim, P. S.; Farmer, M.; Heinrikson, R. L. *Proc. Natl. Acad. Sci. U.S.A.* **1977**, *74*, 2256.
(19) St. Charles, R.; Walz, D. A.; Edwards, B. F. *J. Biol. Chem.* **1989**, *264*, 2092.
(20) Zucker, M. B.; Katz, I. R. *Prog. Biophys. Mol. Biol.* **1991**, *198*, 693.
(21) Ilyina, E.; Milius, R.; Mayo, K. H. *Biochemistry* **1994**, *33*, 13436.
(22) Ilyina, E.; Mayo, K. H. *Biochem. J.* **1995**, *306*, 407.
(23) Lecomte-Raclet, L.; Alemany, M.; Sequira-Le Grand, A.; Amiral, J.; Quentin, G.; Vissac, A. M.; Caen, J. P.; Han, Z. C. *Blood* **1998**, *91*, 2772.
(24) Lecomte-Raclet, L.; Rholam, M.; Alemany, M.; Lazar, N.; Simenel, C.; Delepierre, M.; Han, Z. C.; Cohen, P.; Caen, J. P. *Biochemistry* **2000**, *39*, 9612.
(25) Stewart, J. M.; Young, J. D. *Solid-Phase Peptide Synthesis*, 2nd ed.; Pierce Chemical Co.: Rockford, IL, 1984.
(26) Reed, J.; Reed, T. A. *Anal. Biochem.* **1997**, *254*, 36.
(27) Marini, D. M.; Hwang, W.; Lauffenburger, D. A.; Zhang, S.; Kamm, R. D. *Nano Lett.* **2002**, *2*, 295.
(28) Waterhous, D. V.; Johnson, W. C., Jr. *Biochemistry* **1994**, *33*, 2121.
(29) Greenfield, N.; Fasman, G. D. *Biochemistry* **1969**, *8*, 4108.
(30) Dyson, H. J.; Rance, M.; Houghten, R. A.; Wright, P. E.; Lerner, R. A. *J. Mol. Biol.* **1988**, *201*, 201.
(31) Johnson, W. C., Jr. *Proteins* **1990**, *7*, 205.
(32) Nevskaya, N. A.; Chirgadze, Y. N. *Biopolymers* **1976**, *15*, 637.
(33) Chirgadze, Y. N.; Nevskaya, N. A. *Biopolymers* **1976**, *15*, 627.
(34) Chirgadze, Y. N.; Nevskaya, N. A. *Biopolymers* **1976**, *15*, 607.
(35) Mayo, K. H.; Roongta, V.; Ilyina, E.; Milius, R.; Barker, S.; Quinlan, C.; La Rosa, G.; Daly, T. J. *Biochemistry* **1995**, *34*, 11399.
(36) Menger, F. M.; Venkatasubban, K. S. *J. Org. Chem.* **1978**, *43*, 3143.
(37) Croguennoc, P.; Nicolai, T.; Kuil, M. E.; Hollander, J. G. *J. Phys. Chem. B* **2001**, *105*, 5782.
(38) Capitani, D.; Crescenzi, V.; De Angelis, A. A.; Segre, A. L. *Macromolecules* **2001**, *34*, 4136.
(39) Capitani, D.; De Angelis, A. A.; Crescenzi, V.; Masci, G.; Segre, A. L. *Carbohydr. Polym.* **2001**, *45*, 245.
(40) Renard, D.; Lefebvre, J. *Int. J. Biol. Macromol.* **1992**, *14*, 287.
(41) Dawson, R. M. C.; Elliott, D. C.; Elliott, W. H.; Jones, K. M. *Data for Biochemical Research*, 3rd ed.; Clarendon Press: Oxford, U.K., 1986.
(42) Wüthrich, K. *NMR of Proteins and Nucleic Acids*; John Wiley & Sons: New York, 1986.
(43) Isrealachvili, J. N. *Intermolecular and Surface Forces*, 2nd ed.; Academic Press: San Diego, CA, 1991.
(44) Caplan, M. R.; Moore, P. N.; Zhang, S.; Kamm, R. D.; Lauffenburger, D. A. *Biomacromolecules* **2000**, *1*, 627.
(45) Verwey, E. J. W.; Overbeek, J. T. G. *Theory of Stability of Lyophobic Colloids*; Elsevier: Amsterdam, 1948.
(46) Derjaguin, B. V.; Landau, L. *Acta Physicochim. URSS* **1941**, *14*, 633.

BM025573D